Home   Search   Collections   Journals   About   Contact us   My IOPscience

Strain-tunable band gap of hydrogenated bilayer graphene

You may also be interested in:

Strain-tunable band gap of hydrogenated bilayer graphene

Yang Zhang, Chun-Hua Hu, Yu-Hua Wen[1], Shun-Qing Wu and Zi-Zhong Zhu[1]

Department of Physics and Institute of Theoretical Physics and Astrophysics, Xiamen University, Xiamen 361005, People's Republic of China
E-mail: yhwen@xmu.edu.cn and zzhu@xmu.edu.cn

Abstract. First-principles calculations have been utilized to investigate the biaxial strain-dependent electronic properties of fully hydrogenated bilayer graphene. It has been found that after complete hydrogenation, bilayer graphene exhibits semiconducting characteristics with a wide direct band gap. The band gap can be tuned continuously by the biaxial strain. Furthermore, compressive strain can induce the semiconductor-to-metal transition of this hydrogenated system. The origin of the strain-tunable band gap is discussed. The present study suggests the possibility of tuning the band gap of fully hydrogenated bilayer graphene by using mechanical strain and may provide a promising approach for the fabrication of electromechanical devices based on bilayer graphene.

Contents

[1] Authors to whom correspondence should be addressed.

IOP Institute of Physics ⬧ DEUTSCHE PHYSIKALISCHE GESELLSCHAFT

1. Introduction

Graphene, a two-dimensional (2D) honeycomb monolayer with sp^2 hybridized carbon atoms, has attracted a great deal of interest since its experimental discovery in 2004 [1]. Owing to its novel properties, for example the ultra-high electron mobility, anomalous quantum Hall effect, ballistic transport at room temperature and truly atomic thickness, graphene has been suggested to be a suitable candidate material for next-generation nanoelectronics [2–4]. Because of the tangential π and π^* bands at the Dirac point, pure graphene is a zero-gap semiconductor. Lack of a band gap limits the direct utilization of graphene in nanoelectronic and nanophotonic devices. Therefore, opening or tuning a band gap becomes imperative for the technological application of graphene.

To date, a variety of strategies have been explored in order to engineer the band gap of graphene: for example, surface adsorption [5–10], cutting graphene into a nanoribbon [11], patterning bilayer or even multilayer graphene, utilizing graphene–substrate interaction [12] and applying an external electric field to bilayer graphene [13, 14]. Hydrogenation of graphene has been suggested both theoretically and experimentally to be a promising approach to create a finite band gap [5–8]. For example, fully hydrogenated graphene, in which all carbon atoms are in sp^3 hybridization, is a semiconductor with a wide direct band gap of about 3.5 eV [5–7]. Graphene with half-hydrogenation, however, is a ferromagnetic semiconductor with a narrow indirect band gap of 0.46 eV [8]. Additionally, mechanical strain has been used to engineer the band gap of graphene experimentally [15–18]. A tunable band gap at the Dirac point can be realized by applying uniaxial strain on graphene [15]. The G and 2D band Grüneisen parameters have been yielded by biaxial strain in graphene adhered to a SiO_2/Si substrate [16]. Available theoretical studies have also verified that mechanical strain can significantly modify the electronic properties of carbon nanotubes [19, 20] as well as ZnO and Si nanowires [21, 22].

On the other hand, bilayer graphene has attracted a great deal of attention recently [13, 14, 18, 23–26]. In bilayer graphene, low-energy excitation is one of the characteristics of massive chiral fermions, unlike Dirac fermions in graphene [2]. Most importantly, evidence has been presented that bilayer graphene can provide a strain-tunable band gap and, as such, may suggest a maneuverable approach for the fabrication of electromechanical devices based on bilayer graphene [18, 26].

The aforementioned studies have motivated our study of the effects on bilayer graphene subjected to hydrogenation and mechanical strain. In this paper, we present the corresponding results based on density functional theory (DFT) calculations. Similar to monolayer graphene with full hydrogenation [5–7], fully hydrogenated bilayer graphene (HBG) exhibits semiconducting characteristics. Of particular interest are the strain effects on electronic properties of HBG. We find that the band gap of HBG can be tuned continuously by the strain. Furthermore, compressive strain can lead to the transition of HBG from the semiconducting to the metallic state.
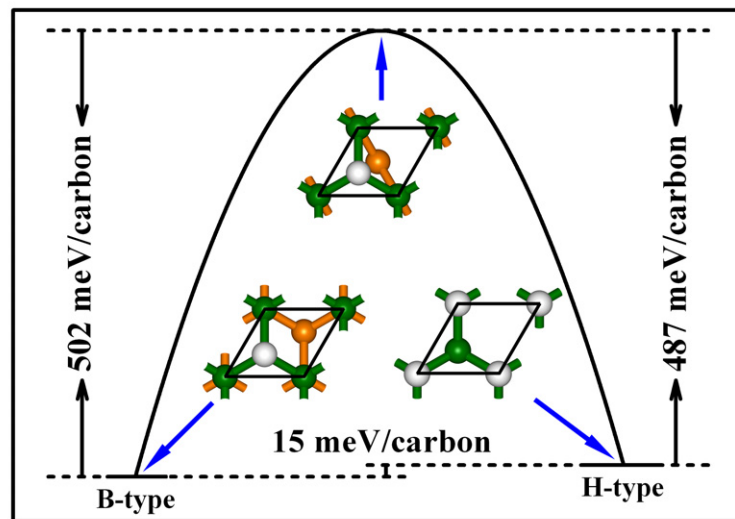
2. Computational method

First-principles calculations based on the spin-polarized DFT within the projector aug-mented wave method [27, 28], as implemented in the Vienna *ab initio* simulation package (VASP) [29, 30], have been employed to investigate the structural and electronic properties
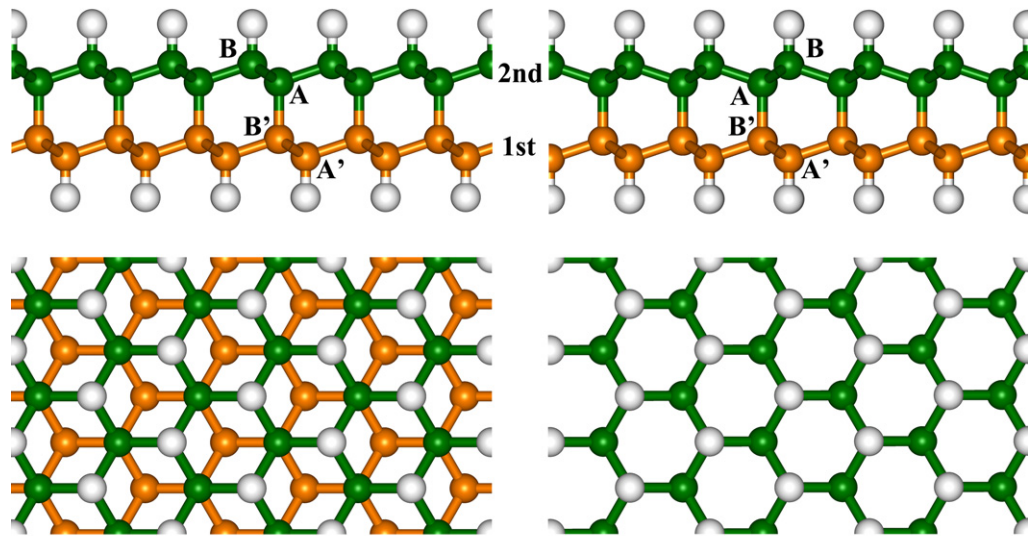
Figure 1. Side and top views of (a) B-type and (b) H-type HBGs. Carbon atoms in the first and second layers are in gold and green, respectively. Hydrogen atoms are in light gray. (c) Energy barriers (unit: meV per carbon atom) between the B- and H-type HBGs. Insets give the homologous configurations in the feasible phase transition path.

of HBG tuned by in-plane biaxial strain. The functional of Perdew and Wang 91 (PW 91) with generalized gradient approximation is used to describe the exchange correlation interactions [31]. The cut-off of plane-wave energy is set to 450 eV, and the convergence for total energy is controlled to be smaller than 10^{-6} eV. An $11 \times 11 \times 1$ k-point mesh with Gamma centered grid is adopted to describe the Brillouin-zone integrations. All the HBGs are located in the x–y plane and modeled in a hexagonal supercell with periodic boundary conditions. Along

Table 1. Properties of HBGs: lattice constant a (Å), average C–C bond lengths within layers d_{C-C} (Å) and between layers D (Å), average C–H bond length d_{C-H} (Å), binding energy per carbon atom E_b (eV) and band gap E_g (eV).

| HBG	a	d_{C-C}	D	d_{C-H}	E_b	E_g
B-type	2.533	1.541	1.561	1.109	−10.971	2.985
H-type	2.526	1.539	1.587	1.107	−10.956	2.825

the z-axis, a vacuum region of at least 10 Å is applied to eliminate the interaction between layers. The geometric relaxations are performed by computing the Hellmann–Feynman (H–F) forces using conjugate gradient algorithm [32]. All atoms in the supercell are allowed to move freely until the H–F force on each atom is smaller than 0.001 eV Å^{-1}. The accuracy of the present approach has been tested by calculating the properties of monolayer graphene. Its semi-metallic feature and C–C bond length of 1.424 Å are in good agreement with the experimental and theoretical results [8, 33, 34].

3. Results and discussion

Because the electronic properties of bilayer graphene are strongly dependent on its geometrical structure [23], two types of HBGs are considered in this study: (i) Bernal stacking (termed B-type), in which one half of the carbon atoms in one layer lie directly above the carbon atoms of the adjacent layer, while the other half that are hydrogenated lie over the centers of hexagonal rings of the adjacent layer (see figure 1(a)); (ii) hexagonal stacking (termed H-type), where all carbon atoms of one layer lie above the carbon atoms of the other layer. In this case, the hydrogenated carbon atoms are located at the same sublattice in both layers (see figure 1(b)).

After the structural relaxation of HBGs, chemical bonding between layers (A–B$'$ sites) stabilizes both B- and H-type configurations, resulting in sp^3 hybridization of all carbon atoms, as shown in figures 1(a) and (b). Their optimized structural parameters and binding energies are summarized in table 1. Obviously, the average C–C (within layers) and C–H bond lengths of B-type are both approximately equal to those of H-type. The interlayer C–C bond length D of B-type, however, is distinctly smaller than that of H-type, indicating that the interlayer chemical bonds of B-type are stronger than those of H-type. Thereby, B-type HBG is more stable than the H-type one, as indicated by the binding energy in table 1. During biaxial loading, the configurations of both B- and H-type HBGs have similar distortions. Their interlayer C–C and C–H bond lengths have no significant variation. The average C–C bond length within layers increases with increasing positive strain, whereas it decreases with increasing negative strain. Figure 1(c) shows the energy barriers between B- and H-type HBGs calculated by using the nudged elastic band (NEB) method [35–38]. The energy barriers from B- to H-type and from H- to B-type are estimated to be 502 and 487 meV per carbon atom, respectively. Owing to the negligible difference in binding energy (15 meV per carbon atom between B- and H-type HBGs) and large energy barriers, both B- and H-type configurations can be regarded as stable states.

Figure 2 illustrates the electronic band structures and band gaps of HBGs as a function of biaxial strain. It can be seen that the HBGs are nonmagnetic semiconductors with direct
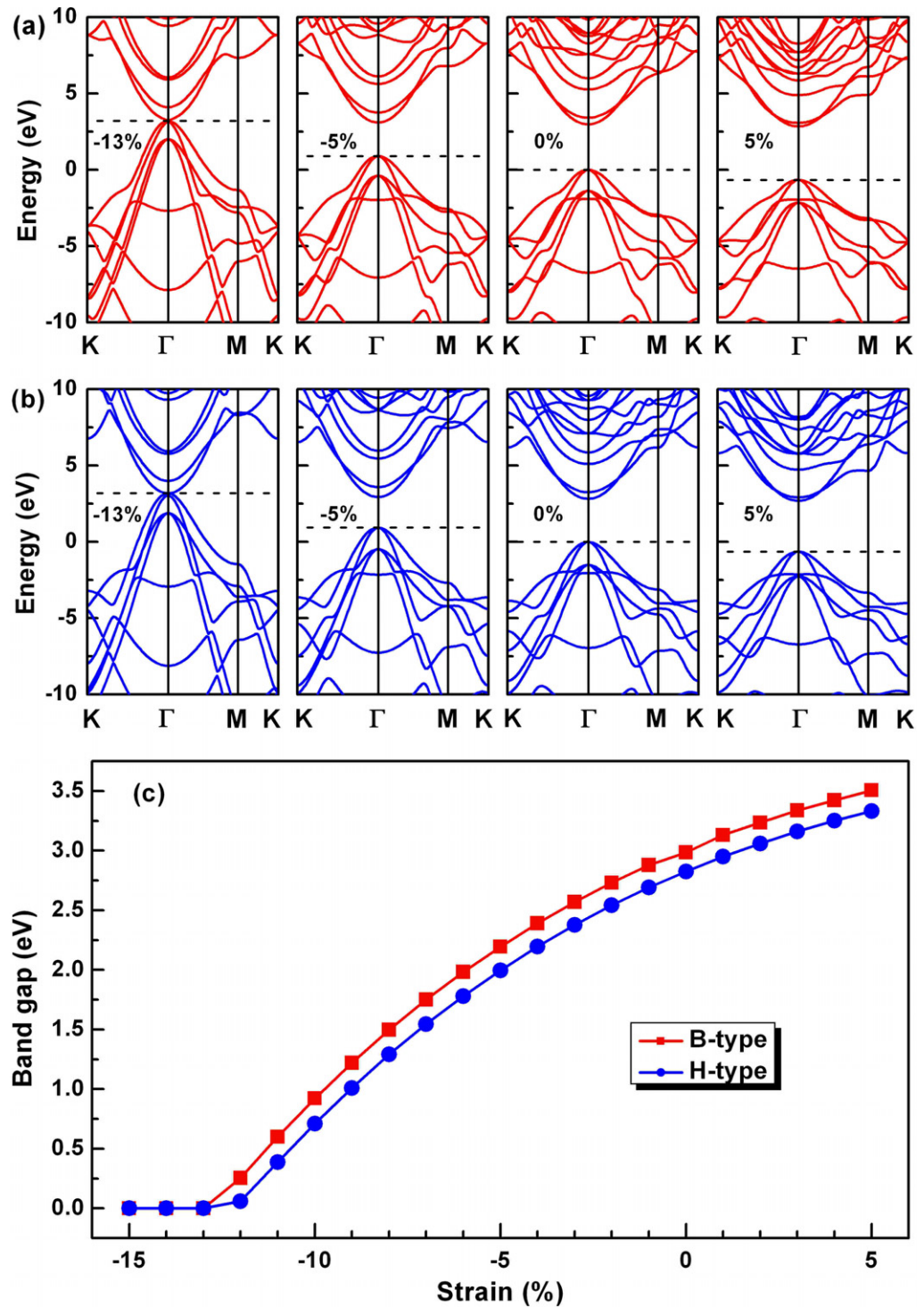
Figure 2. Electronic band structures of (a) B-type and (b) H-type HBGs with different biaxial strains. The zero point of energy in all the band structures is chosen to be the VBM energy of the unstrained bilayer. The dashed line marks the highest occupied level. (c) The band gaps of the HBGs as a function of the biaxial strain.

band gaps of 2.985 and 2.825 eV for the unstrained B- and H-type configurations (see table 1), respectively. More importantly, their band structures under the unstrained state are almost the same (see figures 2(a) and (b)), indicating that their structural differences do not influence the band structures significantly. However, the band structures of the HBGs are strongly dependent on the biaxial strain. By applying a tensile biaxial strain, their band gaps are increased by about 100 meV per 1% stretch, whereas under a compressive strain, they are decreased monotonically from about 2.985 to 0 eV (see figure 2(c)). The critical strain of the transition from semiconducting to metallic state is −13% for both B- and H-type HBGs. To validate the present computing parameters such as the kinetic energy cut-off and k-point mesh, we have also adopted a large energy cutoff of 600 eV and a $21 \times 21 \times 1$ k-point mesh to calculate the binding energy and band structure of strained (−13%) B-type HBG and obtained the same results as those described above.

Why do the HBGs exhibit fantastic electronic properties with biaxial strain? In order to explore the origin of the strain-tunable band gap, we display the partial density of state (PDOS) of B-type HBG under different strains in figure 3. It can be observed from this figure that the valence band maximum (VBM) of the B-type HBG is occupied by p_x and p_y orbitals of all carbon atoms, while the conduction band minimum (CBM) is mainly contributed by p_z orbital of hydrogenated carbon atoms and the s electron of hydrogen atoms. Thereby, the band gap is determined by the energy difference between $E^*_{p_z-s}$ and $E_{p_x-p_y}$, where $E^*_{p_z-s}$ is the anti-bonding energy between p_z orbital of hydrogenated carbon atoms and s orbital of hydrogen atoms, and $E_{(p_x-p_y)}$ is the bonding energy between p_x and p_y orbitals of all carbon atoms. From a comparison of figures 3(a)–(c), it is found that the biaxial strain has no remarkable influence on the anti-bonding state between p_z and s orbitals distributed at CBM. This is because the C–H bond is flexible because of the movability of hydrogen atom with adsorbed carbon atom at the free surfaces. However, the bonding state between p_x and p_y orbitals located at VBM and lower energy range varies dramatically with the biaxial strain and is strengthened with the tensile strain and weakened with the compressive strain. This directly leads to a shift in the energy of VBM to a higher level under the compressive strain (see figure 3(a)) and to a lower one under the tensile strain (see figure 3(c)). Therefore, the band gap of the B-type HBG decreases with the compressive strain and increases with the tensile strain. Finally, a semiconductor-to-metal transition occurs at a strain of about −13%. For the H-type HBG, the tunable band gap and semiconductor-to-metal transition induced by the biaxial strain can also be elucidated in the same formalism.

Generally, mechanical strain modifies the band gaps of semiconductors irregularly, depending on the type of material [21, 22, 39, 40]. For example, the band gap of a Ge layer grown on the Si substrate increases with compressive strain but decreases with tensile strain [39]. For strained anatase TiO_2 bulk, whether the band gap decreases or increases depends on the style of the applied strain [40]. In addition, our previous study shows that the band gap of a ZnO nanowire varies nonmonotonically with uniaxial strain [21]. Nevertheless, the present work reveals that the band gaps of HBGs can be tuned monotonically by biaxial strain.

4. Conclusion

In summary, we have performed DFT calculations to investigate the electronic properties of fully hydrogenated bilayer graphene, and found that hydrogenated bilayers with different configurations exhibit semiconducting characteristics. These particular semiconducting features
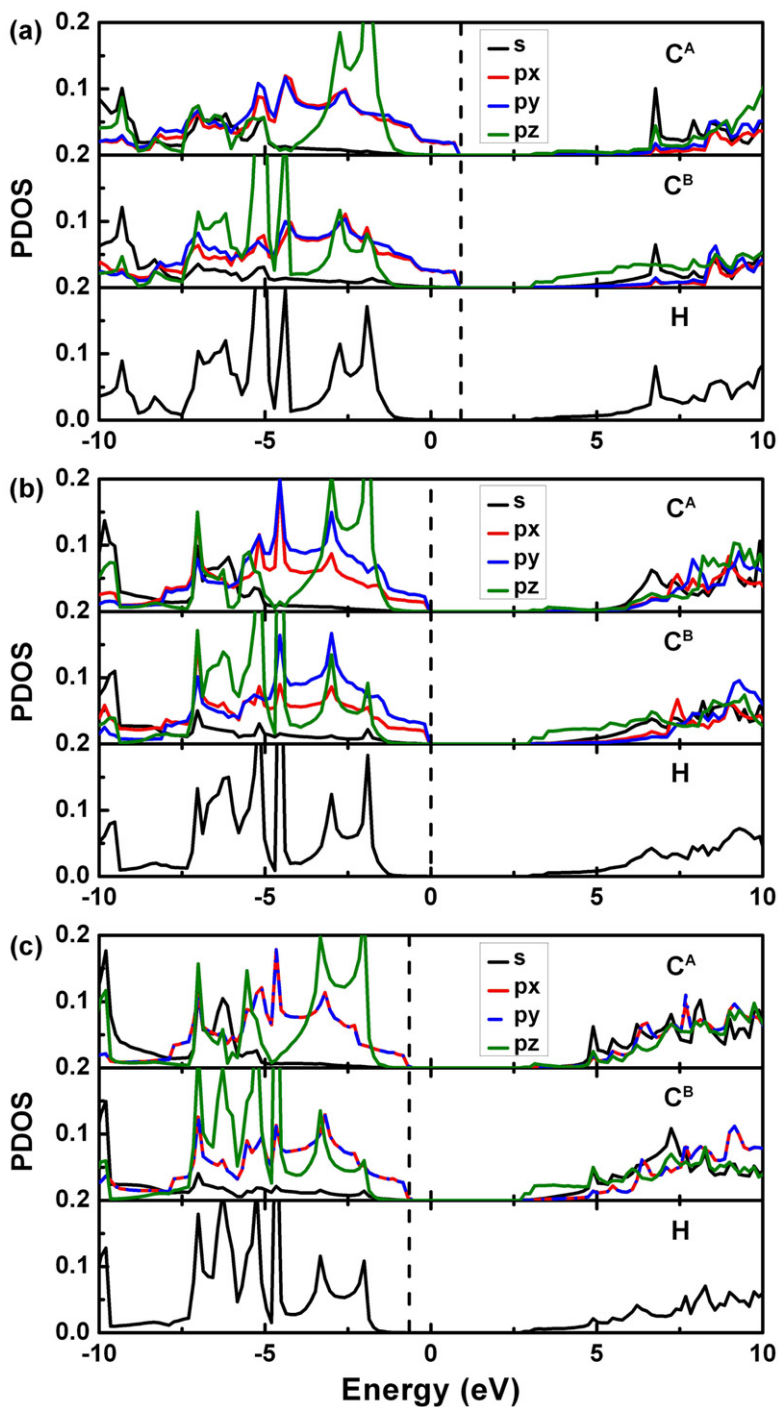
Figure 3. PDOS of B-type HBGs with biaxial strain of (a) −5%, (b) 0% and (c) 5%. The zero point of energy in all the PDOS is chosen to be the VBM energy of unstrained HBG. The dashed line marks the highest occupied level. Owing to the symmetry, the PDOS are shown only for A and B position carbon atoms. C^A and C^B denote the carbon atoms located at A (B′) and B (A′) positions in figure 1, respectively.

IOP Institute of Physics **Φ** DEUTSCHE PHYSIKALISCHE GESELLSCHAFT

result from sp^3 chemical bonding and allow us to tune continuously the band gap with biaxial strain. Compressive strain can induce the transformation of HBGs from the semiconducting to the metallic state. Such a tunable band gap and semiconductor-to-metal transition mainly contribute to the bonding state between p_x and p_y orbitals of carbon atoms and the antibonding state between p_z orbital of hydrogenated carbon atoms and s orbital of hydrogen atoms. The present work suggests that fully hydrogenated bilayer graphene could be fabricated into novel materials with finely tunable band gaps by using mechanical strain.

References

[1] Novoselov K S, Geim A K, Morozov S V, Jiang D, Zhang Y, Dubonos S V, Grigorieva I V and Firsov A A 2004 *Science* **306** 666
[2] Novoselov K S, Geim A K, Morozov S V, Jiang D, Katsnelson M I, Grigorieva I V, Dubonos S V and Firsov A A 2005 *Nature* **438** 197
[3] Zhang Y, Tan Y W, Stormer H L and Kim P 2005 *Nature* **438** 201
[4] Geim A K and Novoselov K S 2007 *Nat. Mater.* **6** 183
[5] Elias D C *et al* 2009 *Science* **323** 610
[6] Sofo J O, Chaudhari A S and Barber G D 2007 *Phys. Rev. B* **75** 153401
[7] Zhou J, Wu M M, Zhou X and Sun Q 2009 *Appl. Phys. Lett.* **95** 103108
[8] Zhou J, Wang Q, Sun Q, Chen X S, Kawazoe Y and Jena P 2009 *Nano Lett.* **9** 3867
[9] Yan J, Xian L and Chou M Y 2009 *Phys. Rev. Lett.* **103** 086802
[10] Wang W L and Kaxiras E 2010 *New J. Phys.* **12** 125012
[11] Han M Y, Ozyilmaz B, Zhang Y B and Kim P 2007 *Phys. Rev. Lett.* **98** 206805
[12] Zhou S Y, Gweon G H, Fedorov A V, First P N, de Heer W A, Lee D H, Guinea F, Castro Neto A H and Lanzara A 2007 *Nat. Mater.* **6** 770
[13] Ohta T, Bostwick A, Seyller T, Horn K and Rotenberg E 2006 *Science* **313** 951
[14] Oostinga J B, Heersche H B, Liu X, Morpurgo A F and Vandersypen L M K 2007 *Nat. Mater.* **7** 151
[15] Ni Z H, Yu T, Lu Y H, Wang Y Y, Feng Y P and Shen Z X 2008 *ACS Nano* **2** 2301
[16] Metzger C, Remi S, Liu M, Kusminskiy S V, Castro Neto A H, Swan A K and Goldberg B B 2010 *Nano Lett.* **10** 6
[17] Ding F, Ji H X, Chen Y H, Herklotz A, Dörr K, Mei Y F, Rastelli A and Schmidt O G 2010 *Nano Lett.* **10** 3453
[18] Choi S M, Jhi S H and Son Y W 2010 *Nano Lett.* **10** 3486
[19] Minot E D, Yaish Y, Sazonova V, Park J Y, Brink M and McEuen P L 2003 *Phys. Rev. Lett.* **90** 156401
[20] Sreekala S, Peng X H, Ajayan P M and Nayak S K 2008 *Phys. Rev. B* **77** 155434
[21] Zhang Y, Wen Y H, Zheng J C and Zhu Z Z 2009 *Appl. Phys. Lett.* **94** 113114
[22] Lu A J, Zhang R Q and Lee S T 2007 *Appl. Phys. Lett.* **91** 263107
[23] Nanda B R K and Satpathy S 2009 *Phys. Rev.* B **80** 165430
[24] Samarakoon D K and Wang X Q 2010 *ACS Nano* **4** 4126
[25] Xia F, Farmer D B, Lin Y and Avouris P 2010 *Nano Lett.* **10** 715
[26] de Andres P L, Ramírez R and Vergés J A 2008 *Phys. Rev. B* **77** 045403
[27] Blöchl P E 1994 *Phys. Rev. B* **50** 17953

[28] Kresse G and Joubert D 1999 *Phys. Rev.* B **59** 1758
[29] Kresse G and Furthmüller J 1996 *Phys. Rev.* B **54** 11169
[30] Kresse G and Furthmüller J 1996 *Comput. Mater. Sci.* **6** 15
[31] Perdew J P, Chevary J A, Vosko S H, Jackson K A, Pederson M R, Singh D J and Fiolhais C 1992 *Phys. Rev.* B **46** 6671
[32] Feynman R P 1939 *Phys. Rev.* **56** 340
[33] Berger C *et al* 2006 *Science* **312** 1191
[34] Castro Neto A H, Guinea F, Peres N M R, Novoselov K S and Geim A K 2009 *Rev. Mod. Phys.* **81** 109
[35] Henkelman G, Uberuaga B P and Jónsson H 2000 *J. Chem. Phys.* **113** 9901
[36] Henkelman G and Jónsson H 2000 *J. Chem. Phys.* **113** 9978
[37] Oviedo O A, Leiva E P M and Mariscal M M 2008 *J. Phys.: Condens. Matter* **20** 265010
[38] Hu C H, Yang Y and Zhu Z Z 2010 *Solid State Commun.* **150** 669
[39] Ishikawa Y, Wada K, Cannon D D, Liu J, Luan H C and Kimerling L C 2003 *Appl. Phys. Lett.* **82** 2044
[40] Yin W J, Chen S Y, Yang J H, Gong X G, Yan Y F and Wei S H 2010 *Appl. Phys. Lett.* **96** 221901